

Anti-Yellowing Property of Polyurethane Improved by the Use of Surface-Modified Nanocrystalline Cellulose

Hao Zhang, Heyu Chen, Ying She, Xue Zheng, and Junwen Pu *

Nanocrystalline cellulose (NCC) was used to improve the anti-yellowing property of polyurethane (PU). The NCC was modified with 3-glycidoxypropyltrimethoxysilane (GPTMS) to enhance its compatibility with PU, and the surface-modified NCC was characterized by contact angle (CA), X-ray powder diffraction (XRD), and thermogravimetric analysis (TG). NCC/PU composite was examined by scanning electron microscopy (SEM), Fourier transform infrared spectrophotometer (FT-IR), and X-ray photoelectron spectroscopy (XPS). Anti-yellowing property of the NCC/PU composite was determined using the Chinese National Standard GB/T 23999-2009. The results showed that the CA between modified NCC and PU was decreased by 26.6% (with 8% GPTMS). The crystal structure of NCC was inconspicuously affected by the surface modification, while the thermal stability of modified NCC was enhanced by 5.5%. The surface-modified NCC particles were homogeneously dispersed in the PU (as shown in the SEM micrographs). FT-IR and O1s XPS survey spectra of NCC/PU composites indicated the oxidation of hydroxyl groups and the production of carbonyl groups, while the photochemical degradation of PU resulting from UV radiation was prevented by the addition of NCC. The anti-yellowing property of the NCC/PU composite with 1.5% surface-modified NCC was increased by 57.7% and the contribution was decreased when the content of modified NCC was 2.0%.

Keywords: Polyurethane (PU); Nanocrystalline cellulose (NCC); Modification; Anti-yellowing

Contact information: College of Materials Science and Technology, Beijing Forestry University, Haidian District, Beijing 100083, PR China; *Corresponding author: pjunwen@126.com

INTRODUCTION

Polyurethane (PU) is one of the most popular polymers for the molecular architectures designed for each application. Abrasion and corrosion resistances are some of the major advantages of PU, while the yellowing of PU, caused by the photochemical degradation resulting from ultraviolet (UV) radiation, greatly affects its optical and mechanical properties (Irusta and Fernandez-Berridi 1999; Rosu *et al.* 2009). Many kinds of UV absorbers have been studied to mitigate the yellowing of PU.

Organic UV absorbers have been synthesized to improve the yellowing of PU for many years (Chu and Fischer 1978). Blends of PU based on 4,4'-dibenzyl diisocyanate with 1,2-bis-[2(2-hydroxy-5-methylphenyl)-5-benzotriazolyl]-ethane as the UV absorber were prepared, and the blend properties were investigated (Scortanu *et al.* 2004). The UV absorbers mixture of UV-531 and UV-327 was prepared to avoid the destruction of PU coating (Wang *et al.* 2013). A mixture of a hindered amine light stabilizer (Tinuvin® 123) and a UV absorber (Tinuvin® 400) was used to protect the PU (Jana and Bhunia 2010).

Inorganic materials have been used as the UV absorbers due to their significant effects (Craciun *et al.* 2011). CeO₂ was used as a UV absorber with PU polymers (Saadat-Monfared *et al.* 2012; Saha *et al.* 2013). TiO₂/ZnO particles and ZnO/CeO₂ particles were used as a mixture of UV absorbers, and the degradation of PU film was reduced distinctly (Sha *et al.* 2011; Ugur *et al.* 2011). ZnO was used to improve the UV resistance and prevent the formation of cracks in PU film (Rashvand *et al.* 2011; Salla *et al.* 2012). The effect of SiO₂ on the protective properties of polyurethane coatings has been investigated (Mills *et al.* 2012).

Compared with the organic and inorganic UV absorbers, nanocrystalline cellulose (NCC) has many advantages, such as environmental compatibility and biodegradability (Zeng *et al.* 2002; Luo *et al.* 2009). The surface hydroxyl groups of NCC are sensitive to UV energy, and the composites synthesized with NCC have attracted much attention on account of their outstanding properties (Hubbe *et al.* 2008; Li *et al.* 2011). The NCC/PU composite has been treated as one of the most promising approaches for improving the anti-yellowing property of PU. The C-O and C-O-Si groups of GPTMS led to the reduction of the surface energy of NCC particles, and the surface modification of NCC by GPTMS was used to improve the compatibility of NCC with PU. Influences of the surface-modified NCC on the anti-yellowing property of PU were investigated in this study.

EXPERIMENTAL

Materials

The NCC raw material was obtained from larch. The original NCC was prepared by use of 35% (w/w) sulfuric acid in a laboratory, and the process of acid hydrolysis was operated at 60 °C (Zhang *et al.* 2013). The length of the NCC particles was 100 to 200 nm, and the diameter was 30 to 60 nm. GPTMS was treated as the surface modifier of NCC, and the modifier was used as received without any further purification. The aromatic PU purchased from LEYI Co. Ltd (China) was a thermosetting resin of linear polyether type. The number-average molecular weight of the PU latex was 110,000, and the solids content was 64.9%. All experiments were conducted in air.

Methods

Pretreatment of NCC

GPTMS was used to modify the original NCC. Four different concentrations of GPTMS in ethanol were used to modify the NCC: 2, 4, 6, and 8% (v/v). The pH of the ethanol was adjusted to within the range of 3 to 4 with hydrochloric acid, and GPTMS was hydrolyzed until the solution turned pellucid. One gram of NCC was modified with 100 mL of 2, 4, 6, and 8% GPTMS solution, and the modifications were conducted at 60 °C for 3 h.

Synthesis of NCC/PU composite

The NCC/PU composite was synthesized with PU and surface-modified NCC. The dried surface-modified NCC was added into the latex of PU at the concentrations of 0.5, 1.0, 1.5, and 2.0% (w/w). To disperse the NCC particles homogeneously, the

composite was homogenized at a pressure of 100 MPa 10 times by a homogenizer from GEA NIRO SOAVI (Italy).

Characterization of modified NCC and NCC/PU composite

The contact angle (CA) between surface-modified NCC and PU was investigated with an optical contact angle-measuring instrument from DATAPHYSICS (Germany). PU latex was used as the contact liquid. The NCC film (with a diameter of 1.0 cm) was prepared with 0.2 g dried NCC and pressed at 8.0 MPa. A PU droplet was deposited on the surface of NCC film, and the droplet shape was recorded. The contact angles were measured using the image analysis software, and the experimental results were the average values of six measurements made on different areas of the film surface. The crystal structure of the surface-modified NCC was examined by use of an X-ray diffractometer (XRD) from SHIMADZU (Japan) with a scan speed of 2°/min. The patterns were obtained within a 5 to 40° 2 θ angular interval with 0.05° step. The crystallinities of modified NCC were calculated as the ratio of the intensity differences in the peak positions. The thermal behavior of the modified NCC was detected with a thermogravimetric analysis (TG) device from SHIMADZU (Japan) at a constant heating rate (10 °C/min) in flowing air from 50 °C to 500 °C.

The state of dispersion of the modified NCC in the NCC/PU composite was analyzed with a HITACHI (Japan) scanning electron microscope (SEM). Samples were mounted on conductive adhesive tape, sputter coated with gold, and observed using a voltage of 15 KV. The ingredients of the pure PU and NCC/PU composite were characterized by a Fourier transform infrared spectrophotometer (FT-IR) from BRUKER (Germany). The scan was operated in the range of 4000 to 400 cm⁻¹ with an accumulation of 64 scans at a resolution of 4 cm⁻¹. The surface examination of the NCC/PU composite was carried out with an X-ray photoelectron spectrometer (XPS) from KRATOS (England). The anode of the XPS was Al, and the step size was 1000.0 meV. The anti-yellowing property of the NCC/PU composite was measured by the Chinese National Standard GB/T 23999-2009 method. According to this method, coatings of the pure PU and NCC/PU composites were treated with constant UV radiation at 60±3 °C for 168 h, and the radiation intensity was 0.68 W/m² (340 nm). The coatings treated with UV radiation were compared with the control group, and ΔE (measured by the colorimeter) was used to indicate the yellowing of samples with different contents of surface-modified NCC.

RESULTS AND DISCUSSION

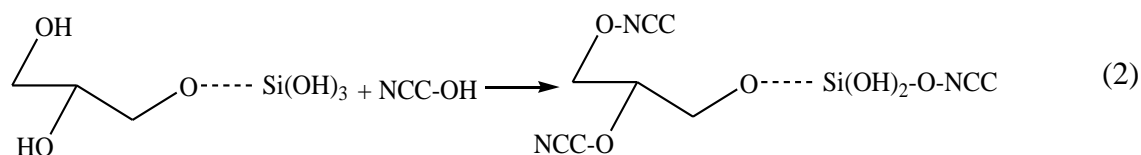
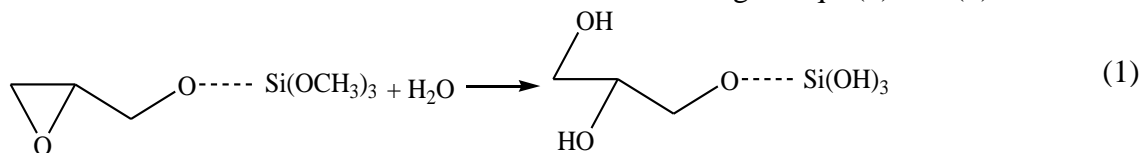
Tests of NCC Modified by GPTMS

Examination of compatibility of modified NCC with PU

The compatibility of surface-modified NCC with PU was indicated by CA, and the surface modification effect of GPTMS on the compatibility of NCC particles is shown in Fig. 1.

The silanol groups were obtained through the hydrolyzing of alkyl-oxygen groups of GPTMS. The surface of original NCC was abundantly covered with hydroxyl groups. And the hydroxyl groups of NCC were substituted by the hydrolyzed GPTMS, with the formation of stable covalent bonds. The structure of NCC was restrained by the chains

from GPTMS, which were presented as a cross-linked network between the PU and surface-modified NCC. These can be illustrated according to Eqs. (1) and (2) as follows:



Eqs. 1 and 2. Modification of NCC with GPTMS

Compatibility of the surface-modified NCC with PU, influenced by the lipophilic groups from GPTMS, increased significantly. As indicated in Fig. 1, the CA between original NCC and PU was 84.9° . With the 4% GPTMS treatment, the CA of modified NCC was decreased to 67.4° . The enhancement of the compatibility slowed down as the content of GPTMS increased. Compared with the control group, CA between the surface-modified NCC and PU was decreased by 26.6% when 8% GPTMS was used. The molecular structure of GPTMS was filled with C-O-Si groups, which led to the reduction of the surface energy of NCC. The epoxy groups from GPTMS can produce obvious space resistance and the hydroxyl groups of NCC were displaced by the C-O from the epoxy groups. It is known that the CA is affected by the surface energy and the linkages within the composite materials led to a lower surface energy.

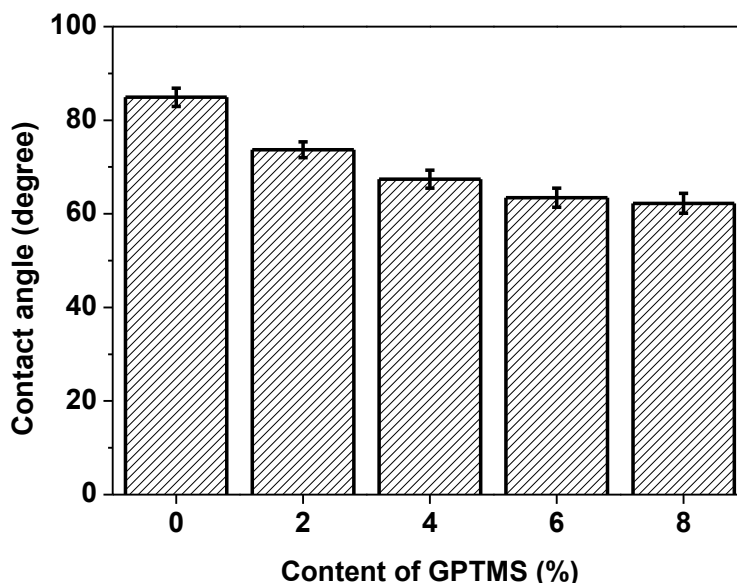


Fig. 1. CA between surface-modified NCC and PU

Crystal structure of original and surface-modified NCC

The XRD patterns and crystallinities of the original and surface-modified NCC are shown in Fig. 2 and Table 1, respectively. Diffraction peaks at $2\theta = 16.2^\circ$ and 22.7°

were assigned to the (101) and (002) planes of type I cellulose. The diffraction peak ($2\theta = 20.2^\circ$), as the typical diffraction pattern of cellulose type II, was observed because the crystal structure of NCC was affected by the acid hydrolysis.

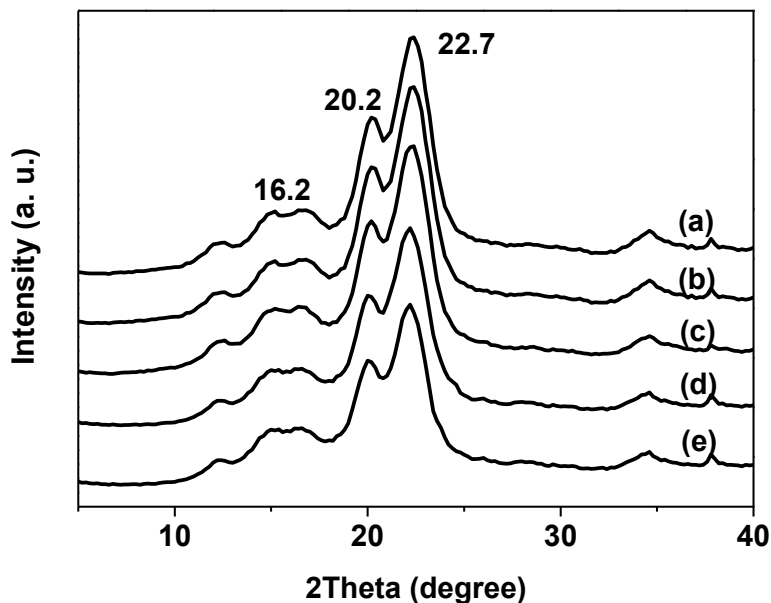


Fig. 2. XRD patterns: (a) original NCC; (b) NCC modified by 2% GPTMS; (c) NCC modified by 4% GPTMS; (d) NCC modified by 6% GPTMS; (e) NCC modified by 8% GPTMS

Compared with the control group shown in Fig. 2a, the XRD diffraction positions of modified NCC were steady. The diffraction intensity of the peak at $2\theta = 22.7^\circ$ was decreased with the enhancement of GPTMS, whereas the intensity of the (101) plane ($2\theta = 16.2^\circ$) was marginally influenced (indicated in Fig. 2). The crystal regions of NCC were affected by GPTMS, and the crystallinity of the surface-modified NCC showed a slight reduction after the surface-modification.

Table 1. Crystallinity of Modified NCC

Sample	a	b	c	d	e
Crystallinity (%)	56.8	55.2	53.1	50.8	49.5

Analysis of thermal stability

Different pretreatments have different influences on the thermal stability of NCC (Eyholzer *et al.* 2010). The thermal behavior of the NCC modified by GPTMS was further investigated by TG. TG curves shown in Fig. 3 indicated that significant weight loss of the surface-modified NCC occurred as the temperature was increased from 290 °C to 320 °C. The loss was attributed to the thermal degradation of the modified NCC. As GPTMS content increased, the TG peak of NCC was raised from 296.4 °C to 312.8 °C (shown in Fig. 3).

The thermal stability of modified NCC decreased significantly when the content of GPTMS was more than 4%. When the content of GPTMS was 8%, the weight loss temperature of surface-modified NCC was 297.6 °C.

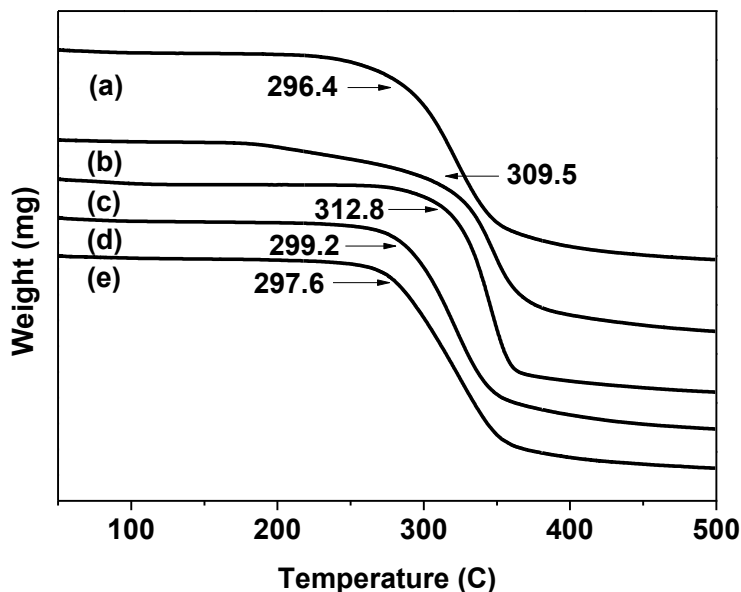


Fig. 3. TG curves: (a) original NCC; (b) NCC modified by 2% GPTMS; (c) NCC modified by 4% GPTMS; (d) NCC modified by 6% GPTMS; (e) NCC modified by 8% GPTMS

Characterizations of the NCC/PU Composite

Disperse state of the surface-modified NCC in PU

The hydroxyl groups of NCC were replaced by the hydrolyzed GPTMS during the process of surface modification, and the state of dispersion of the surface-modified nano particles in PU was improved.

A structural schematic of the NCC/PU composite is presented in Fig. 4. The modified NCC particles were dispersed by a homogenizer, while the structure of PU was disturbed.

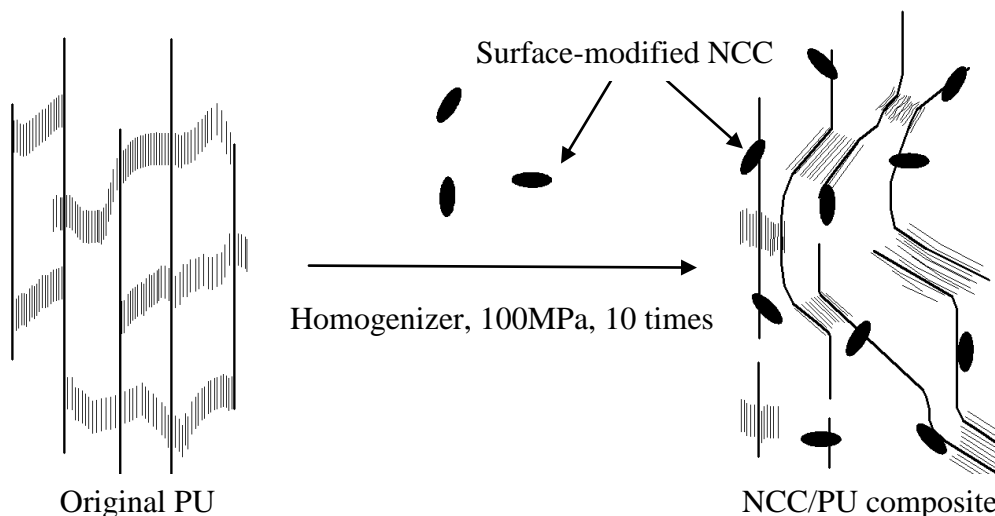


Fig. 4. Structural schematic of the NCC/PU composite

The state of dispersion of the surface-modified NCC (with 8% GPTMS) in the NCC/PU composite was analyzed with SEM; the micrographs of the composite are shown in Fig. 5. Figures 5a and b presented the morphologies of the PU with 0.5% and 1.0% surface-modified NCC, respectively. And the dispersion of the nanoparticles in the NCC/PU composites was uniform.

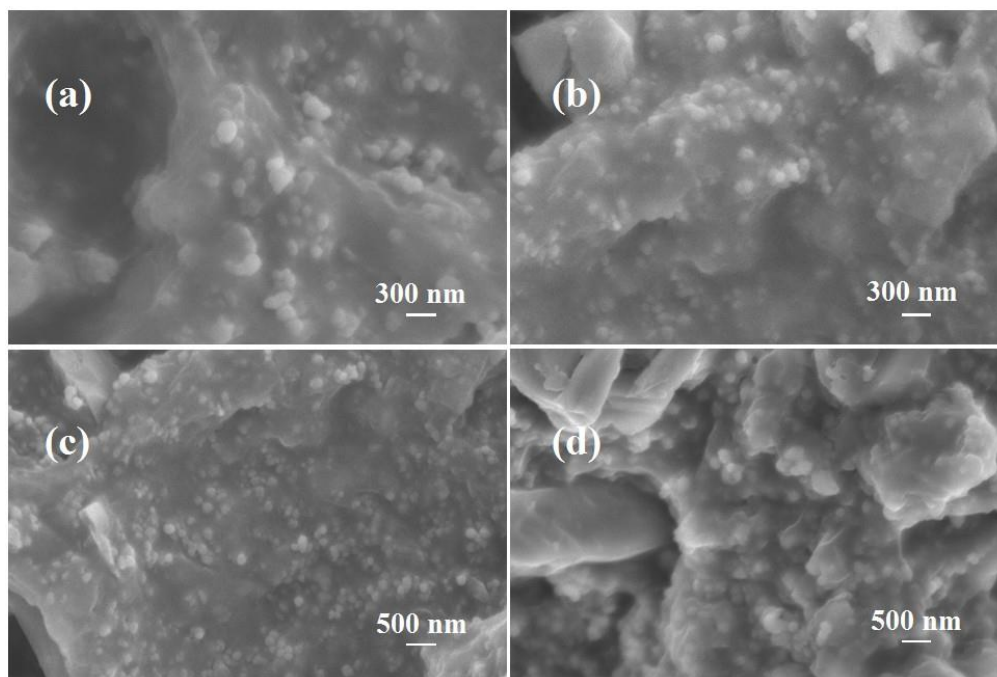


Fig. 5. SEM micrographs of the NCC/PU composite: (a) 0.5% surface-modified NCC; (b) 1.0% surface-modified NCC; (c) 1.5% surface-modified NCC; (d) 2.0% surface-modified NCC

The morphology of the composite was affected by the concentrations of NCC particles significantly. As shown in Fig. 5c, the homogeneous dispersion of the modified nano particles in the NCC/PU composite synthesized with 1.5% modified NCC was visible, while the agglomeration of the surface-modified nano particles existed in the NCC/PU composite when the content of modified NCC was 2.0% (shown in Fig. 5d).

FT-IR spectra of the NCC/PU composite

The structures of the original PU, the control untreated NCC/PU composite, and the NCC/PU composite treated with UV radiation were confirmed by FT-IR, as shown in Fig. 6. The FT-IR spectrum of the original PU (Fig. 6a) showed a peak at 3350 cm^{-1} , which corresponded to the stretching mode of the imino groups; the peak at 2885 cm^{-1} belonged to the asymmetrically stretching vibration of C-H; the absorption peak at 1728 cm^{-1} was attributed to the carbonyl groups; and the bands at 1135 cm^{-1} and 1456 cm^{-1} were related to the stretching vibration of C-O-C. With the addition of NCC, the absorption peak at 3430 cm^{-1} was observed, as seen in Fig. 6b. The emergence of the peak at 3430 cm^{-1} indicated that hydroxyl groups were introduced into the NCC/PU composite.

As shown in Fig. 6c, the absorption peak at 3430 cm^{-1} of the sample treated with UV radiation decreased significantly, and the absorption peak at 1728 cm^{-1} was greatly

enhanced. These results showed that the hydroxyl groups of NCC in the NCC/PU composite were oxidized by the UV radiation, and carbonyl groups were produced. The relatively steady characteristic absorption peaks at 1135 cm^{-1} , 1456 cm^{-1} , 2885 cm^{-1} , and 3350 cm^{-1} revealed that the photochemical decomposition of PU that usually would take place due to the UV energy was prevented by the addition of NCC.

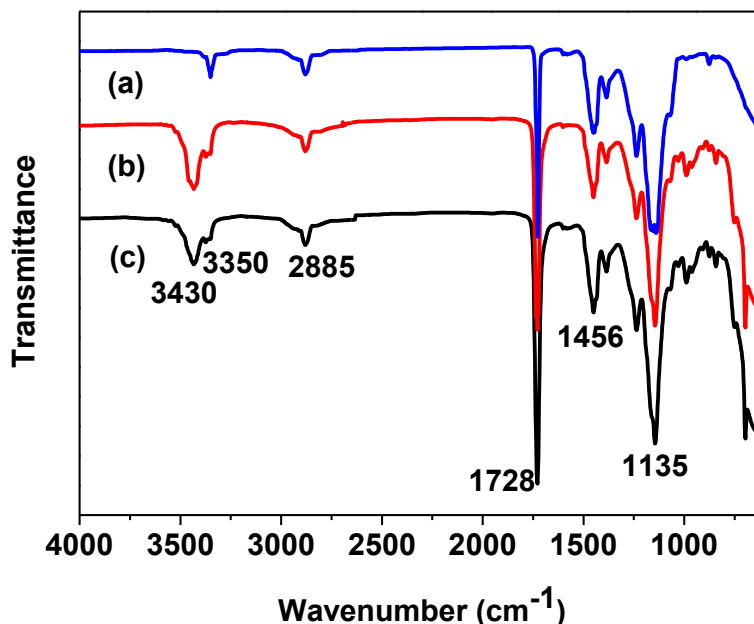


Fig. 6. FT-IR spectra: (a) original PU; (b) control untreated group of NCC/PU composite; and (c) NCC/PU composite treated with UV radiation

Surface analysis of the NCC/PU composite

Typical O1s XPS survey spectra of the NCC/PU composite are presented in Fig. 7. The O0 fraction at 530.35 eV is associated with the carbonyl groups, and the O1 at 531.99 eV represents ether-type oxygen. The C-OH linkages are indicated by the O2 peak at 533.41 eV (Barry and Koran 1990).

Compared with the curves of control group presented in Fig. 7A, the XPS survey spectra of NCC/PU composite were affected by the UV radiation significantly (shown in Fig. 7B). The obvious decrease of O2 peak indicated that the hydroxyl groups of NCC were oxidized by UV radiation and the carbonyl groups were generated (indicated by the enhancement of O0 peak) during the process of UV treatment. The relatively steady O1 peak showed that the ether bonds of PU was damaged by UV rays limitedly and this phenomenon indicated that the photochemical degradation of PU resulted from the UV radiation was inhibited by addition of NCC.

According to the surface compositions of NCC/PU composite reported in Table 2, the content of O2 was decreased from 9.56% to 7.92% for the oxidation of hydroxyl groups, while the production of carbonyl groups led to the increase of O0 from 0.67% to 3.47%. The insignificant reduction of O1 content from 13.48% to 12.88% indicated the stability of ether bonds of PU.

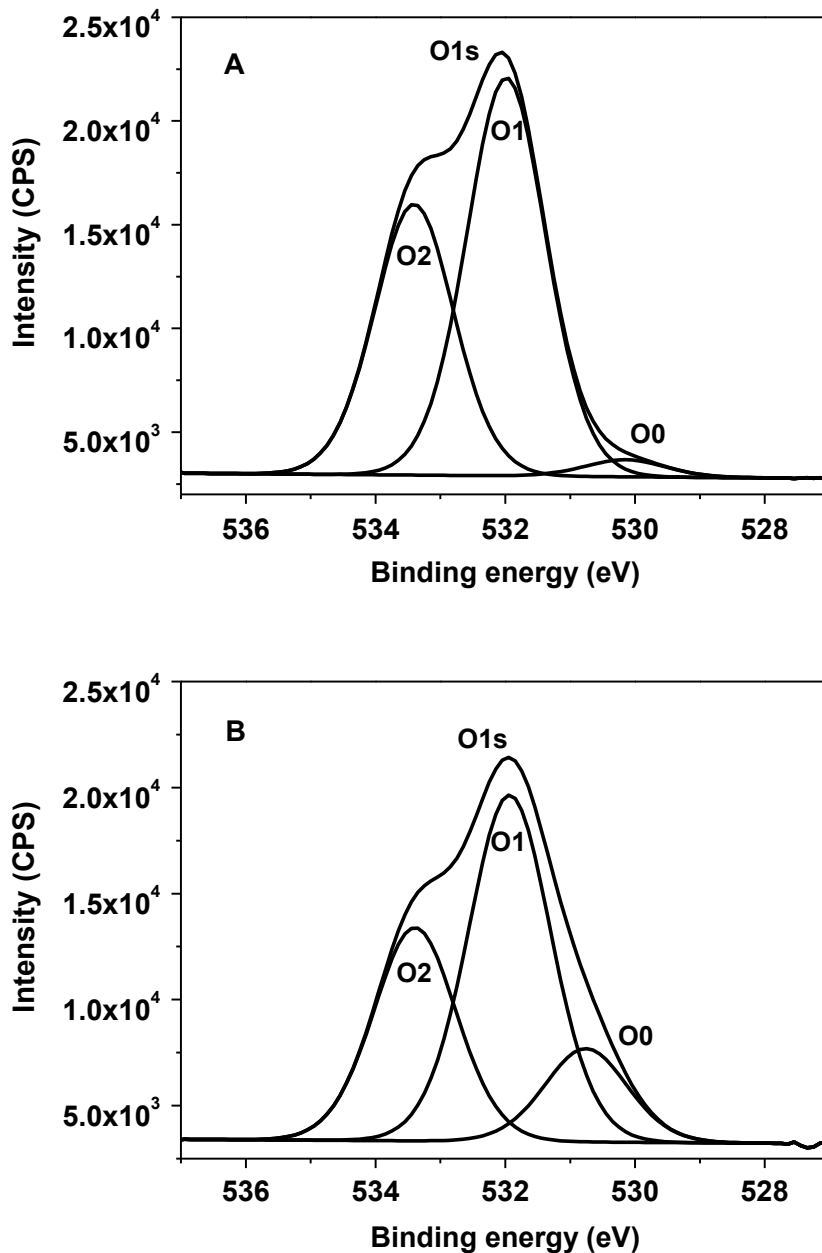


Fig. 7. O1s XPS survey spectra: (A) control untreated group of NCC/PU composite; (B) NCC/PU composite treated with UV radiation

Table 2. Summary of O1s XPS Results for NCC/PU Composite

Samples	Surface concentration (%)			
	O1s	O0	O1	O2
Control untreated	23.71	0.67	13.48	9.56
UV radiation treated	24.27	3.47	12.88	7.92

Anti-yellowing property of the NCC/PU composite

The photochemical degradation of PU is associated with the scission of the urethane group and photooxidation of the central CH₂ group between the aromatic rings. These reactions are combined with the yellowing of PU. The addition of surface-modified NCC led to the inhibition of photochemical degradation of PU, and the anti-yellowing property of NCC/PU composite was improved. The relationship between the amount of modified NCC used and the yellowing of the NCC/PU composite is shown in Fig. 8.

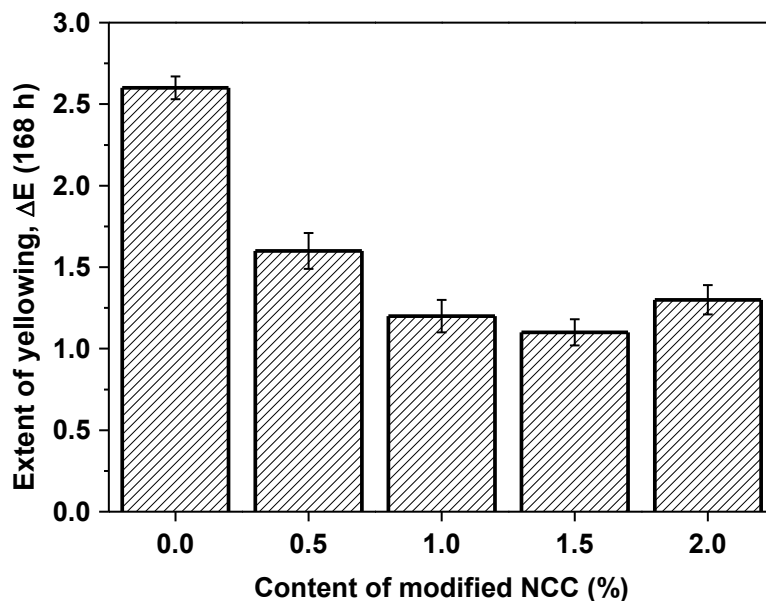


Fig. 8. Extent of yellowing (168 h of UV irradiation) of NCC/PU composite

Yellowing of the original PU resulting from the UV radiation was conspicuous. When the content of surface-modified NCC was 1.0%, the ΔE of the NCC/PU composite decreased from 2.6 of the pure PU to 1.2. The reduction of ΔE indicated the improvement of the anti-yellowing property of NCC/PU composite, and the growth rate of anti-yellowing slowed down as the NCC concentration increased. Compared with the pure PU, the anti-yellowing property of the NCC/PU composite synthesized with 1.5% surface-modified NCC increased by 57.7%. It was obvious that the incremental contribution to the anti-yellowing property decreased when the content of modified NCC was 2.0%.

CONCLUSIONS

1. GPTMS was used to modify the original NCC, and the compatibility of surface-modified NCC with PU was increased by 26.6% (when the concentration of GPTMS was 8%). GPTMS affected the XRD diffraction peak of NCC at $2\theta = 22.7^\circ$ more obviously than the peak at $2\theta = 16.2^\circ$, and the crystallinities of the nanoparticles were reduced by surface modification slightly. The weight loss temperature of surface-modified NCC was increased from 296.4 °C of control group to 312.8 °C with 4% GPTMS.

2. From the SEM micrographs of NCC/PU composite it can be concluded that the state of dispersion of the surface-modified NCC in PU was homogeneous. The FT-IR and O1s XPS survey spectra of the NCC/PU composite indicated that the photochemical decomposition of PU was prevented by the addition of NCC.
3. The anti-yellowing property of NCC/PU composite was affected by the surface-modified NCC significantly. The yellowing of the composite was decreased by 57.7% with 1.5% surface-modified NCC, while the incremental contribution to the anti-yellowing property decreased when the content of modified NCC was 2.0%.

ACKNOWLEDGEMENTS

The authors were supported by “the Fundamental Research Funds for the Central Universities” (NO. BLYJ201301) and the Forestry Industry Research Special Funds for Public Welfare Projects: Research and Demonstration of Fast-growing Wood Modification and Application (201204702-B2).

REFERENCES CITED

- Barry, A. O., and Koran, Z. (1990). “Surface analysis by ESCA of sulfite post-treated CTMP,” *J. Appl. Polym. Sci.* 39(1), 31-42.
- Chu, C. C., and Fischer, T. E. (1978). “Evaluation of sunlight stability of polyurethane elastomers for maxillofacial use. I,” *J. Biomed. Mater. Res.* 12(3), 347-359.
- Craciun, E., Ioncea, A., Jitaru, I., Covaliu, C., and Zaharescu, T. (2011). “Nano oxides UV protectors for transparent organic coatings,” *Rev. Chim-Bucharest.* 62(1), 21-26.
- Eyholzer, C., Bordeanu, N., Lopez-Suevos, F., Rentsch, D., Zimmermann, T., and Oksman, K. (2010). “Preparation and characterization of water-redispersible nanofibrillated cellulose in powder form,” *Cellulose* 17(1), 19-30.
- Hubbe, M. A., Rojas, O. J., Lucia, L. A., and Sain, M. (2008). “Cellulosic nanocomposites: A review,” *BioResources* 3(3), 929-980.
- Irusta, L., and Fernandez-Berridi, M. J. (1999). “Photooxidative behaviour of segmented aliphatic polyurethanes,” *Polym. Degrad. Stabil.* 63(1), 113-119.
- Jana, R. N., and Bhunia, H. (2010). “Accelerated hygrothermal and UV aging of thermoplastic polyurethanes,” *High Perform. Polym.* 22(1), 3-15.
- Li, Y., Ren, H. F., and Ragauskas, A. J. (2011). “Rigid polyurethane foam/cellulose whisker nanocomposites: preparation, characterization, and properties,” *J. Nanosci. Nanotechnol.* 11(8), 6904-6911.
- Luo, X. G., Liu, S. L., Zhou, J. P., and Zhang, L. N. (2009). “In situ synthesis of Fe₃O₄/cellulose microspheres with magnetic-induced protein delivery,” *J. Mater. Chem.* 19(21), 3538-3545.
- Mills, D. J., Jamali, S. S., and Paprocka, K. (2012). “Investigation into the effect of nano-silica on the protective properties of polyurethane coatings,” *Surf. Coat Tech.* 209:137-142.
- Rashvand, M., Ranjbar, Z., and Rastegar, S. (2011). “Nano zinc oxide as a UV-stabilizer for aromatic polyurethane coatings,” *Prog. Org. Coat.* 71(4), 362-368.

- Rosu, D., Rosu, L., and Cascaval, C. N. (2009). "IR-change and yellowing of polyurethane as a result of UV irradiation," *Polym. Degrad. Stabil.* 94(4), 591-596.
- Saadat-Monfared, A., Mohseni, M., and Tabatabaei, M. H. (2012). "Polyurethane nanocomposite films containing nano-cerium oxide as UV absorber. Part 1. Static and dynamic light scattering, small angle neutron scattering and optical studies," *Colloid. Surface A.* 408:64-70.
- Saha, S., Kocaefe, D., Boluk, Y., and Pichette, A. (2013). "Surface degradation of CeO₂ stabilized acrylic polyurethane coated thermally treated jack pine during accelerated weathering," *Appl. Surf. Sci.* 276(1), 86-94.
- Salla, J., Pandey, K. K., and Srinivas, K. (2012). "Improvement of UV resistance of wood surfaces by using ZnO Nanoparticles," *Polym. Degrad. Stabil.* 97(4), 592-596.
- Scortanu, E., Priscariu, C., and Caraculacu, A. A. (2004). "Study of the mechanical properties of dibenzyl-based polyurethane containing a molecularly dispersed UV absorber," *High Perform. Polym.* 16(1), 113-121.
- Sha, S., Kocaefe, D., Krause, C., and Larouche, T. (2011). "Effect of titania and zinc oxide particles on acrylic polyurethane coating performance," *Prog. Org. Coat.* 70(4), 170-177.
- Ugur, S. S., Sariisik, M., and Aktas, A. H. (2011). "Nano-TiO₂ based multilayer film deposition on cotton fabrics for UV-protection," *Fiber Polym.* 12(2), 190-196.
- Wang, Y. Z., Wang, H. Y., Li, X. S., Liu, D. X., Jiang, Y. F., and Sun, Z. H. (2013). "O₃/UV synergistic aging of polyester polyurethane film modified by composite UV absorber," *J. Nanomater.* 2013, 169405.
- Zeng, H., Li, J., Liu, J. P., Wang, Z. L., and Sun, S. H. (2002). "Exchange-coupled nanocomposite magnets by nanoparticle self-assembly," *Nature* 420(6914), 395-398.
- Zhang, H., She, Y., Song, S. P., Lang, Q., and Pu, J. W. (2013). "Particulate reinforcement and formaldehyde adsorption of modified nanocrystalline cellulose in urea-formaldehyde resin adhesive," *J. Adhes. Sci. Technol.* 27(9), 1023-1031.

Article submitted: September 1, 2013; Peer review completed: November 6, 2013;
Revised version received: December 4, 2013; Accepted: December 5, 2013; Published:
December 10, 2013.